water

MDPI

Article

Photodegradation of Methylene Blue Using a UV/H_2O_2 Irradiation System

Mohammad Ashraf Ali, Ibrahim M. Maafa * and Isam Y. Qudsieh

Department of Chemical Engineering, College of Engineering, Jazan University, Jazan 45142, Saudi Arabia; mashrafali@jazanu.edu.sa (M.A.A.); isamyq@jazanu.edu.sa (I.Y.Q.)
* Correspondence: imoaafa@jazanu.edu.sa

Abstract: This study presents an efficient way to degrade methylene blue (MB) present in water via photodegradation using H_2O_2 as an oxidant in the presence of UV irradiation and without the use of a catalyst. The reaction variables, employed to evaluate the performance of the photodegradation process using the UV/H_2O_2 system, were the amount of H_2O_2 in the reacting solution and the initial concentration of methylene blue. The degradation of methylene blue in the presence of H_2O_2 was not observed during agitation in darkness. The degradation time decreased as the H_2O_2 concentration increased after the ideal concentration was reached. At this stage, as it began to scavenge the generated hydroxyl radicals, the rate of degradation became inversely proportional to the concentration of H_2O_2. An increase in the quantities of MB and H_2O_2 improved the degradation efficiency because the oxidation process was aided by using the appropriate amount of H_2O_2 and an ideal length of UV light exposure. The experimental data obtained were well-fitted to zero-order reaction kinetics based on the high values of the correlation coefficient. It is believed that the OH radicals ($OH^{\bullet}$) generated during the breakdown of H_2O_2 and the generated $O_2^{\bullet-}$ species attack the MB molecules and produce MB radicals ($MB^{\bullet}$). These MB radicals further experience oxidation and convert to intermediates and finally to CO_2 and H_2O. The UV/H_2O_2 system proved to be quite efficient for the photodegradation of methylene blue without the use of any solid catalyst. This UV/H_2O_2 system can be employed in the degradation of other organic pollutants in industrial wastewater.

Keywords: photodegradation; methylene blue; UV/H_2O_2 irradiation system; zero-order reaction kinetics

Citation: Ali, M.A.; Maafa, I.M.; Qudsieh, I.Y. Photodegradation of Methylene Blue Using a UV/H_2O_2 Irradiation System. *Water* **2024**, *16*, 453. https://doi.org/10.3390/w16030453

Academic Editors: Laura Bulgariu, Cristina Palet and Julio Bastos-Arrieta

Received: 14 December 2023
Revised: 28 January 2024
Accepted: 29 January 2024
Published: 30 January 2024

1. Introduction

Methylene blue (MB) is a colored cationic organic compound that is used as a commercial dye dissolved in water for printing cotton, wool, and silk. The industries produce large volumes of hazardous wastewater, adversely affecting our environment. These effluents contain organic species, such as MB, that harm human health and the environment. Various health hazards are associated with MB, such as nausea, vomiting, mental disorders, and damage to the human eyes [1]. MB is quite stable in the environment, and it is difficult to biodegrade it [2]. The ultimate solution to get rid of this pollutant from wastewater is photodegradation. In photodegradation, a light source interacts with a molecule and causes a chemical change in it. During this process, at least two reactions must occur at the same time: oxidation from photogenerated holes and reduction from photogenerated electrons [3].

Several studies have been conducted and are in progress to either remove MB via adsorption from wastewater or degrade the pollutant into smaller and less hazardous molecules and then finally convert it into water and carbon dioxide. Several studies have utilized H_2O_2 to enhance MB degradation, with or without a semiconductor catalyst. The usage of H_2O_2 accomplishes two purposes; it acts as a strong oxidant and an electron scavenger that prevents electron–hole recombination at the semiconductor surface. Phuc et al. [4] synthesized a ternary composite material, $MgFe_2O_4$–TiO_2/rGO, and achieved

95% efficiency in MB photodegradation under UV and visible light. Ersöz and Altintas [5] used Ag-doped ZnO nanofibers for the photodegradation of MB and concluded that adding H_2O_2 to the process produces reactive OH radicals that enhance MB degradation. Hanadi et al. [6] reported the photolysis of MB using a UV/H_2O_2 system and achieved 100% efficiency of MB degradation. Cao et al. [7] synthesized $ZnFe_2O_4$/$BiVO_4$ nanocomposites for MB photodegradation. They concluded that adding H_2O_2 to the reaction system significantly improved MB degradation due to the generation of OH radicals. Ahad et al. [8] investigated ZnO nanostructures for the photocatalytic degradation of MB. They concluded that H_2O_2 has a significant synergetic effect on photocatalytic activity as an electron scavenger agent. El-Sheshtawy et al. [9] synthesized activated H_2O_2 on the surface of Ag/SiO_2 NPs immobilized on $SrWO_4$ and used it for MB photodegradation. The interaction between Ag/SiO_2 and $SrWO_4$ led to a high catalytic improvement due to the activation of H_2O_2 surface molecules in the absence of light. The catalyst exhibited high catalytic activity over a wide pH range of 4–10. Waimbo et al. [10] utilized nanostructured $CuWO_4$ for the degradation of MB and achieved a 70% conversion in 240 min. Due to the addition of H_2O_2, which acts as an electron-capturing agent, MB degradation was completed within 30 min. Wang et al. [11] prepared a one-dimensional [Cu(tba)$_2$(H_2O)]2H_2O complex and conducted a successful photodegradation of MB. The addition of H_2O_2 enhanced the MB degradation efficiency of the complex. Shi et al. [12] synthesized different GO/polythiophene composites and used them for the photodegradation of MB. The presence of H_2O_2 in the reaction mixture enhanced MB degradation due to the formation of hydroxyl free radicals. Zhang et al. [13] utilized PVDF/GO/ZnO composite membranes for MB photodegradation while using H_2O_2 as an electron-trapping agent. The radical-trapping experiments showed that the oxidizing species (O_2^-) plays an important role in MB degradation. Wang et al. [14] fabricated graphitic carbon nitrides (g-C_3N_4) and utilized them for MB photodegradation under visible light. They observed that H_2O_2 addition significantly enhanced MB photodecomposition. Liu et al. [15] synthesized α-Fe_2O_3 nanoparticles with different sizes and used them for MB photodegradation; when they added H_2O_2 to the system, the photocatalytic efficiency increased to more than 90% due to the generation of highly oxidative OH radicals. AbulKalam et al. [16] prepared cobalt ferrites ($CoFe_2O_4$) and used them for MB photodegradation with H_2O_2/visible light. The presence of H_2O_2 significantly enhanced the reaction towards MB mineralization. Banerjee et al. [17] used rGO-Fe_3O_4-TiO_2 nanocomposite for the photocatalytic degradation of MB under visible and UV light. The catalyst performed better in UV light (99% of MB degraded) than in visible light (94%). The addition of H_2O_2 provided highly reactive hydroxyl ions that efficiently degraded the MB molecules. Liu et al. [18] concluded that a complex formed between H_2O_2 and TiO_2 hydrosols significantly exhibited enhanced visible light photocatalytic activity for MB degradation. Gao et al. [19] synthesized a Cu_2Se hexagonal nanoplate array film on a Cu substrate at room temperature. When H_2O_2 was added to the reaction, the catalyst exhibited a high photocatalytic degradation of MB. Zhang et al. [20] reported MB photodegradation under UV irradiation using TiO_2 and then adding H_2O_2; they found that the H_2O_2 addition significantly enhanced MB degradation. Shu et al. [21] used H_2O_2 in the photodegradation of wastewater pollutants such as diclofenac, gemfibrozil, ibuprofen, and caffeine with UV irradiation. They found enhanced degradation rates due to the generation of OH radicals. Jiang et al. [22] used MWCNTs/TiO_2 composites for MB photodegradation and observed enhanced MB degradation by adding H_2O_2 as an electron acceptor. Yao and Wang [23] investigated the photocatalytic degradation of MB with TiO_2 and UV irradiation. They concluded that adding H_2O_2 to TiO_2 produces an increased MB degradation effect. Pouretedal and Kadkhodaie [24] utilized CeO_2 nanoparticles for the photodegradation of MB under UV and sunlight irradiation. Adding H_2O_2 advanced the degradation towards completion. Zou et al. [25] utilized amorphous TiO_2 with H_2O_2 and achieved higher MB photodegradation under both visible light and UV irradiation. Andronic and Duta [26] reported the photocatalytic activities of TiO_2 thin film for the photodegradation of MB. They found that H_2O_2 addition enhanced MB photodegradation due to the formation of OH

radicals. Banat et al. [27] investigated the photodegradation of MB under UV irradiation and H_2O_2. The presence of acetone further increased MB degradation due to photosensitization. Bessy et al. [28] prepared barium-doped magnesium ferrite [Ba_x $Mg_{0.8-x}$ Fe_2O_4 (x = 0.2–0.6)] NPs with metal nitrates and egg white solution and achieved the degradation of Congo red and MB under UV irradiation. Thilagavathi et al. [29] synthesized pure WO_3 NPs and WO_3/$NiWO_4$ (having Ni 5 to 20 wt%) nanocomposites and used them for MB photodegradation. Their study achieved the highest degradation of about 90% for 20 wt% Ni in 80 min under UV irradiation.

Some recently published papers have been discussed here to provide an understanding of the latest trends in catalysis for MB photodegradation. Ahmad et al. [30] synthesized MgO NPs that exhibited 90% MB degradation in 120 min of visible light irradiation. Alahmadi et al. [31] performed a hydrothermal synthesis of Bi_2O_3/$MoSe_2$ nanocomposite and used it for MB photodegradation. The Bi_2O_3/$MoSe_2$ nanocomposite exhibited an MB photocatalytic degradation efficiency of 96.5% in 80 min of visible light irradiation. The increased photocatalytic activity was attributed to the high crystallinity and surface area, as well as the small particle size of the catalyst. Abdullah et al. [32] synthesized a ternary CuO/CuS/MnO_2 nanocomposite that showed 98% MB degradation under visible light irradiation in 160 min. Zyoud et al. [33] synthesized a 10% Ag-doped ZnO catalyst and achieved higher MB photodegradation at 444.5 nm irradiation as compared to ZnO. Zhao et al. [34] synthesized ZnO nanoflower arrays (ZnO NFAs), in which the ZnO nanorods were grown vertically downward and formed ZnO NFAs. Different ZnO NFAs synthesized were used for MB degradation, and it was observed that the MB degradation efficiency of ZnO NFAs was enhanced with increasing synthesis times of ZnO NFAs. Basalius et al. [35] reported the use of Ag NPs to achieve 80% photocatalytic degradation of MB in 120 min of sunlight. Al-Attar et al. [36] adopted a green approach to prepare a ternary ZnO/CuO/Al_2O_3 nanocomposite (ratio 3:1:1) with a mean particle size of around 40 nm using the pulsed laser ablation method. They employed it as a photocatalyst to degrade MB at a pH of 10.37. They achieved an MB degradation efficiency of 98.6% within 15 min of irradiation, with a rate constant of 0.2265/min. Jin et al. [37] utilized TiO_2 decorated with 3.0 wt% N-doped carbon quantum dots and reported a visible light MB photodegradation rate of 93.1% in 60 min which was 2.25 times greater than that of pristine TiO_2. Elanthamilan et al. [38] used M-type magnetic strontium hexaferrite ($SrFe_{12}O_{19}$) microspheres and showed 90.2% MB degradation efficiency with higher recyclability. Fu et al. [39] used iron (II) carbonate mineral as a catalyst and reported that 99.7% of MB was degraded in 480 min at a pH of 7.0, an H_2O_2 dosage of 122.38 mM, and a reaction temperature of 25 °C using 2.5 g/L of mineral. Chahar et al. [40] reported the use of Mg^{2+}-substituted Co-Zn nanoferrite particles of the composition $Co_{0.5}Zn_{0.5}MgFeO_4$ having good magnetic properties and achieved complete MB photodegradation in one hour of visible light irradiation. Waheed et al. [41] synthesized CNFO/g-C_3N_4 heterojunction photocatalyst and accomplished an MB photodegradation efficiency of 97.2% in 3 h under solar light irradiation, which was twofold greater than g-C_3N_4. Chen et al. [42] synthesized a ternary novel composite ($SrAl_2O_4$:$Eu^{2+}Dy^{3+}$/g-C_3N_4@NH_2-UiO-66) and accomplished complete photocatalytic degradation of MB within 30 min of irradiation. Sun et al. [43] synthesized Co-doped bimetallic MIL-88B(Fe/Co) and activated potassium persulfate that showed 100% MB removal in 15 min. Javed et al. [44] used cobalt-doped tin oxide Co-SnO_2 NPs and Co-SnO_2/sulfur-doped graphitic carbon nitride (SGCN) NCs under sunlight. The Co-SnO_2/SGCN (50%) nanocomposite exhibited a significant increase in MB degradation and achieved 96% MB degradation in 150 min of sunlight irradiation. Fallatah et al. [45] synthesized spinel MOF material using the hydrothermal method and achieved a photocatalytic degradation efficiency of 94.25% for rhodamine B and 90.52% for crystal violet. Hussain et al. [46] biosynthesized olive fruit extract-based zinc oxide (ZnO@OFE) NPs and achieved 75% and 87% photocatalytic degradation of MB and methyl orange (MO) under sunlight irradiation within 180 min. Negash et al. [47] synthesized reduced graphene oxide (rGO), zinc oxide (ZnO), and reduced graphene oxide-zinc oxide (rGO@ZnO) to

achieve efficient photodegradation of MB. The photocatalytic degradation of MB was performed using direct sunlight irradiation. Using optimum conditions, the MB photocatalytic degradation efficiency achieved was 66%, 96.5%, and 99.0%, and the rate constants were 2.16×10^{-3} min^{-1}, 4.97×10^{-3} min^{-1}, and 5.03×10^{-3} min^{-1}, for rGO, ZnO, and rGO@ZnO nanocatalysts, respectively. This study also has the advantage of using a low amount of catalyst (20 mg) for achieving efficient MB photodegradation. Naffeti et al. [48] conducted a study to synthesize green, economical, and novel bismuth-altered silicon nanowires (Bi@SiNWs) for the photocatalytic degradation of MB using UV and solar irradiations. Bi@SiNWs showed remarkable photocatalytic ability for the degradation of MB up to 44% and 89% under UV and solar irradiation, respectively, within 120 min. Recyclability runs showed strong reusability and photostability of the Bi@SiNWs composite. Ighalo et al. [49] developed a review and reported several techniques used for the mitigation of clofibric acid pollution via adsorption. The studies cited above agree on the enhancing effect that H_2O_2 has on MB photodegradation in the presence of semiconductor catalysts. We utilized UV irradiation with H_2O_2 in this study to perform MB degradation. The parameters tested were the variable concentrations of H_2O_2 and MB in the irradiated solution. This study aimed to use a simple method of photolysis in combination with an oxidant, H_2O_2, to perform the photodegradation of MB without using expensive catalytic materials which need lots of time, effort, and resources for their preparation and characterization. In addition, after the reaction, the catalyst particle be separated using a high-speed centrifuge from the irradiated solution to determine the amount of unreacted MB, which is quite difficult. Figure 1 shows photos of MB in solid and solution form along with its molecular structure.

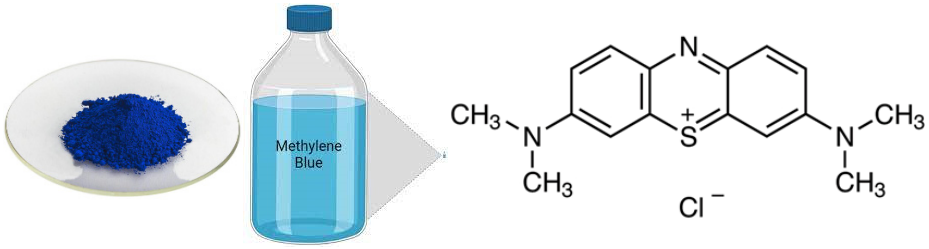

Figure 1. Methylene blue dye as a solid and in solution form, along with its molecular structure.

2. Materials and Methods

2.1. Materials

The chemicals used in this study were MB dye, a 30% hydrogen peroxide (H_2O_2) solution, and drinking water.

2.2. Methods

MB solutions were prepared in drinking water at 5, 10, and 15 ppm concentrations. 100 mL of MB solution from each concentration was taken in separate glass beakers, and a known amount of 30% H_2O_2 solution was added to the beakers and stirred for 20 min in the dark. This step was performed to monitor the degradation of MB with H_2O_2 in the dark. Then, the mixture was irradiated with UV light under continuous agitation. The UV/H_2O_2 reaction system used in this study is shown in Figure 2, equipped with 6W-intensity UV light. The temperature of the solution was maintained at 30 °C during the irradiation process. Every 20 min, 5 mL of the solution was withdrawn from the beaker. A UV–visible spectrophotometer was used to measure the absorbance of the solution at a wavelength of 656 nm (λ_{max} for MB) to monitor the presence of MB. The absorbance of all MB samples exposed to UV radiation was measured for 20 to 80 min. The absorbance data were converted to MB concentration, which remained unconverted in the solution, from which the percent degradation of MB was calculated. The parameters studied were the variable concentration of H_2O_2 (5, 10, and 15 mL) and the concentration of MB (5 ppm, 10 ppm, and 15 ppm) in the reacting solution.

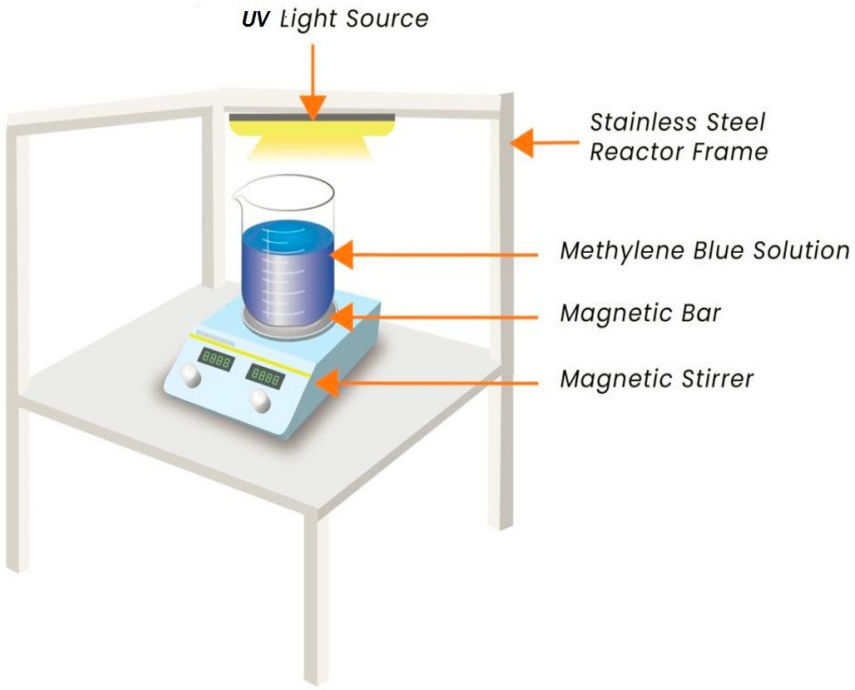

Figure 2. The UV/H_2O_2 reaction system used in this study.

3. Results and Discussion

3.1. Effect of the Amount/Concentration of H_2O_2 in the Reacting Solution

The effect of different amounts of H_2O_2 (5, 10, and 15 mL) on the photocatalytic degradation of MB was investigated. It was observed that MB degradation increased with increasing amounts of H_2O_2 solution and UV irradiation time. Figure 3 shows the percent degradation of MB for the variable amount of H_2O_2. The 15 mL H_2O_2 solution (green) exhibited higher MB degradation compared to the 10 mL (red) and 5 mL H_2O_2 solutions (blue).

3.2. Effect of Initial MB Concentration

The effect of the initial MB dye concentration on the degradation efficiency was investigated by varying the MB dye concentration to 5, 10, and 15 ppm. As shown in Figure 3, at lower MB concentrations (Figure 3A), a higher MB degradation was observed as compared to those in higher MB concentrations (Figure 3B,C). A higher amount of H_2O_2 was quite helpful in the complete degradation of MB. A higher degradation of MB was observed in the reaction solutions having 5 and 10 ppm MB as compared to those having 15 ppm MB. The best and highest degradation trend was observed for 5 ppm MB solution, using 15 mL of H_2O_2 solution.

3.3. Kinetics of MB Photodegradation

The kinetics of the reaction were determined by developing three types of plots, as follows:

(1) C_t/C_o versus time (linear for a zero-order reaction), rate = k;
(2) ln (C_t/C_o) versus time (linear for a first-order reaction), rate = $k[C_t]$;
(3) $1/(C_t/C_o)$ versus time (linear for a second-order reaction), rate = $k[C_t]^2$.

These plots were observed for straight line and correlation coefficient values. Out of the three types of plots (Figures 4–6), the plot of C_t/C_o vs. irradiation time (Figure 4) yielded the highest correlation coefficient values and the best straight-line equation, in which the slope of the equation symbolized the rate constant, k, min^{-1}. This implies that the kinetics of the MB photodegradation reaction are zero-order using the UV/H_2O_2 reaction system. The trends in Figure 4 are similar to those in Figure 3. The data plotted in Figure 5 are the natural logs of C_t/C_o values, while the data plotted in Figure 6 are the inverses of C_t/C_o.

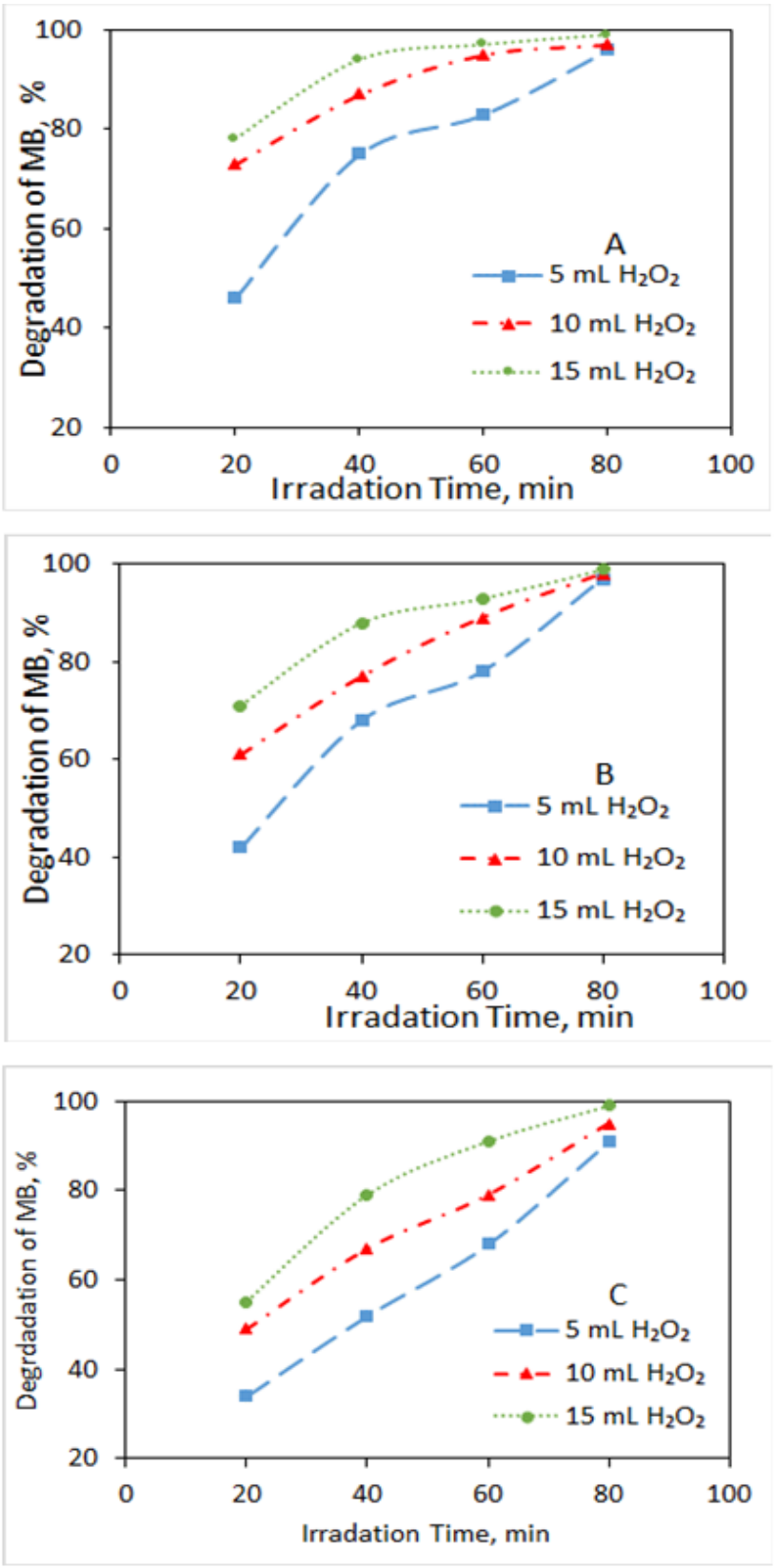

Figure 3. Percent degradation of MB for the initial MB concentration and the variable amount of 30% H_2O_2 solution. Blue line (5 mL 30% H_2O_2 solution), red line (10 mL 30% H_2O_2 solution), and green line (15 mL 30% H_2O_2 solution). (**A**) = 5 ppm MB solution, (**B**) = 10 ppm MB solution, and (**C**) = 15 ppm MB solution.

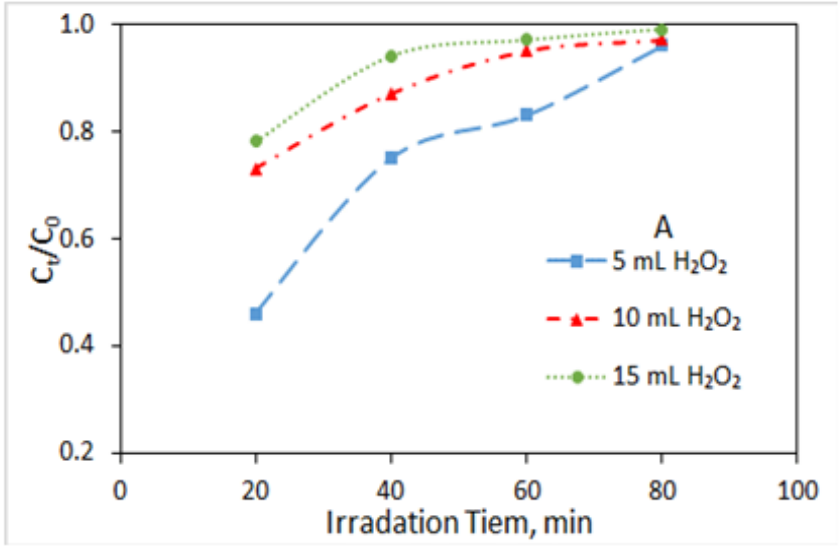

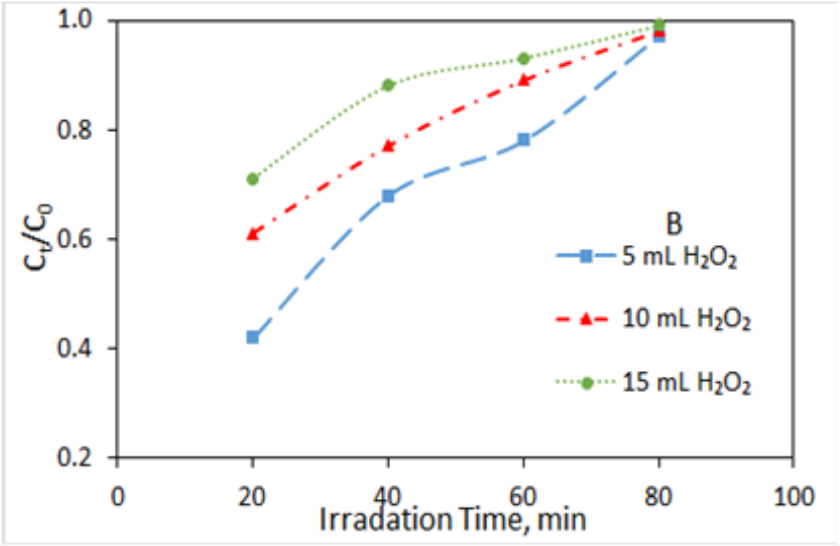

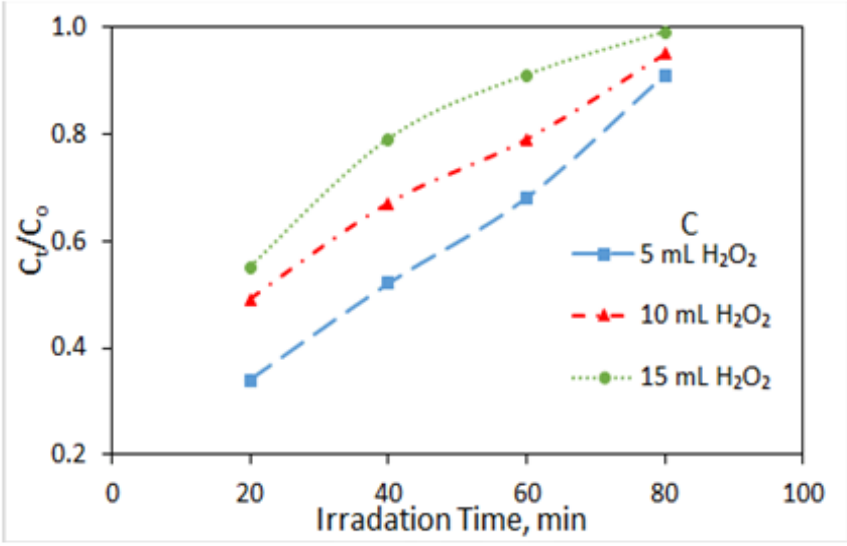

Figure 4. The plots of (C_t/C_o) vs. irradiation time for the zero-order reaction kinetics. Blue line (5 mL 30% H_2O_2 solution), red line (10 mL 30% H_2O_2 solution), and green line (15 mL 30% H_2O_2 solution). (**A**) = 5 ppm MB solution, (**B**) = 10 ppm MB solution, and (**C**) = 15 ppm MB solution.

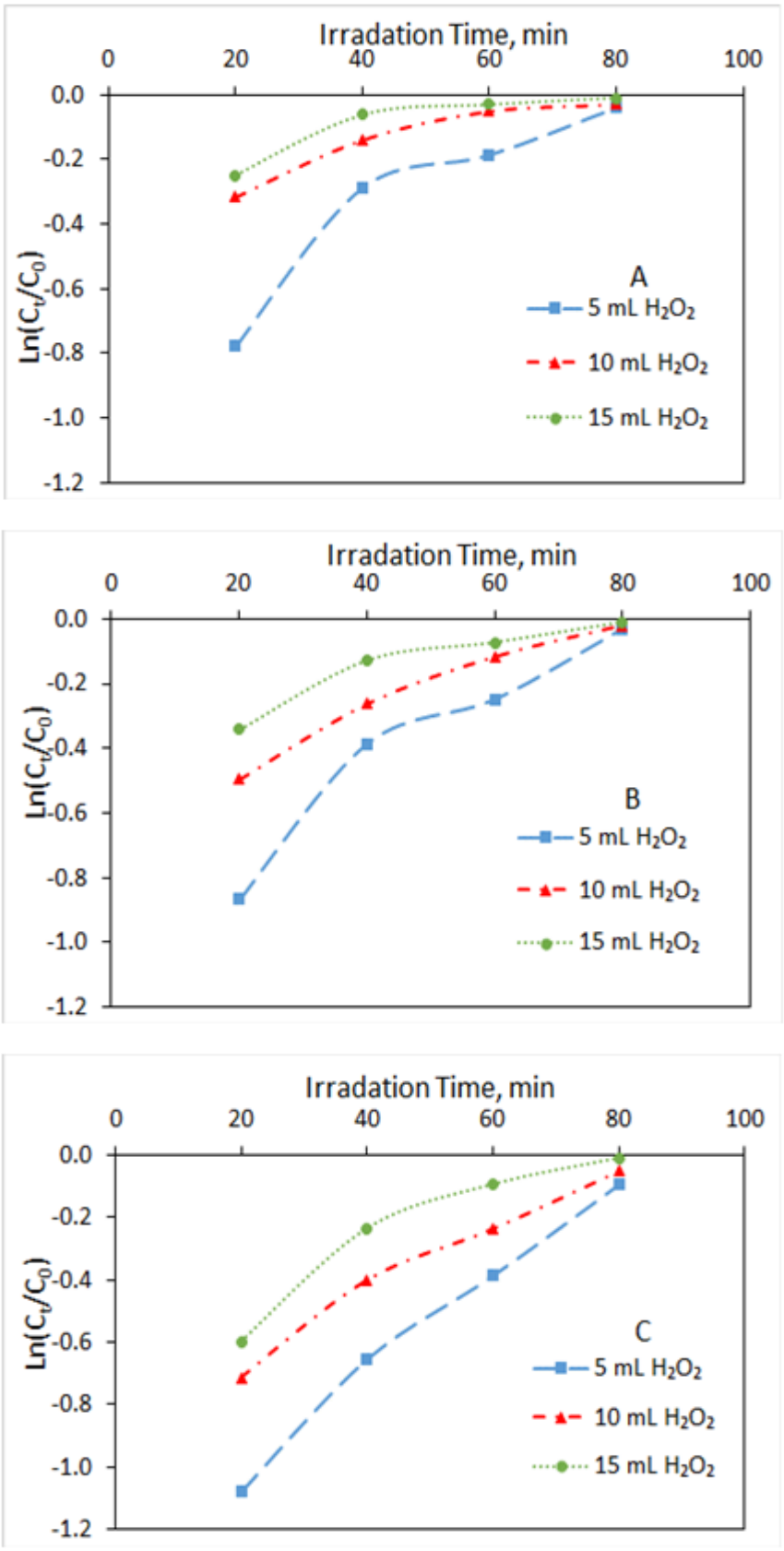

Figure 5. The plots of Ln (C_t/C_0) vs. irradiation time for the first-order reaction kinetics. Blue line (5 mL 30% H_2O_2 solution), red line (10 mL 30% H_2O_2 solution), and green line (15 mL 30% H_2O_2 solution). (**A**) = 5 ppm MB solution, (**B**) = 10 ppm MB solution, and (**C**) = 15 ppm MB solution.

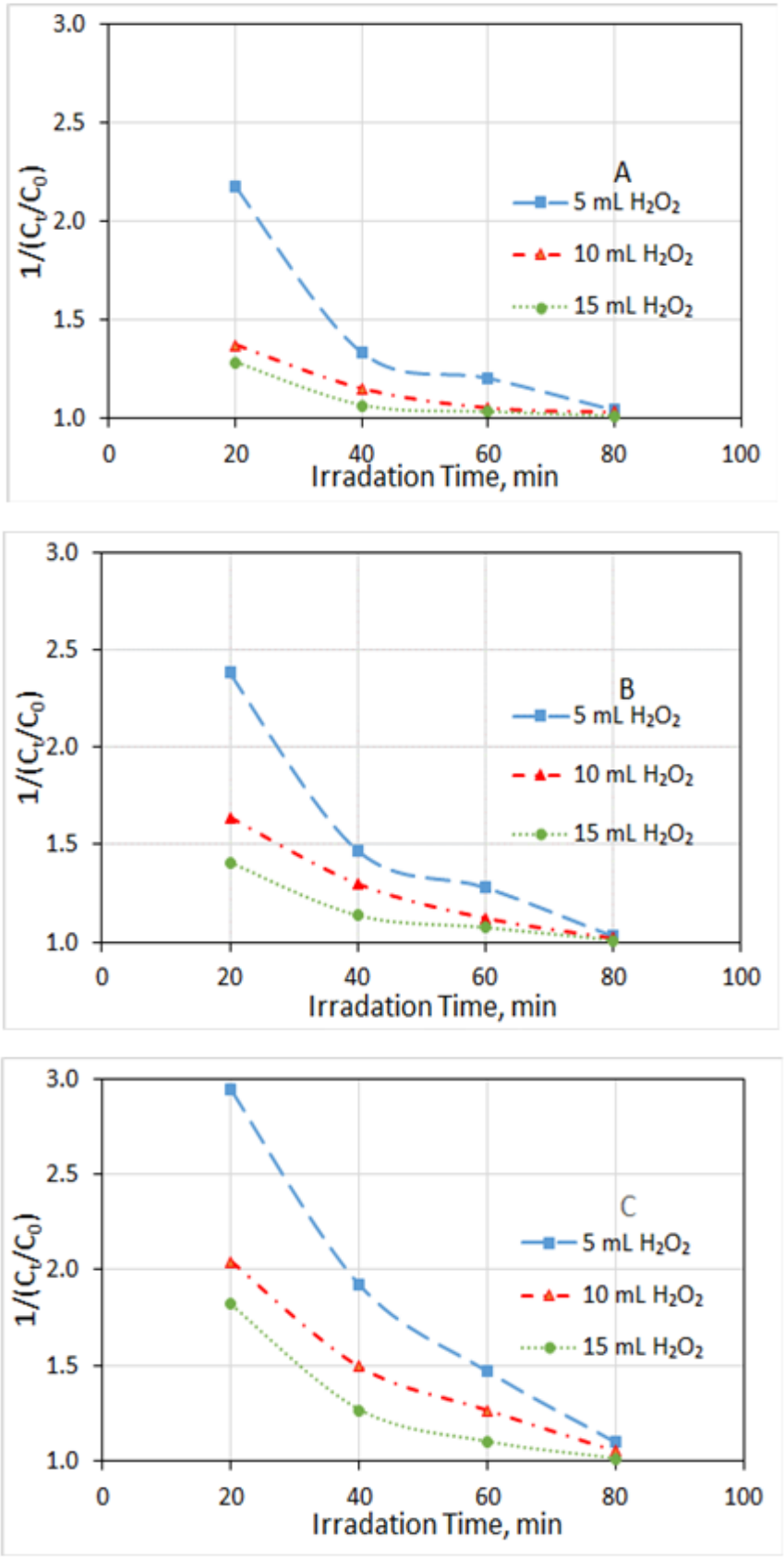

Figure 6. The plots of $1/(C_t/C_o)$ vs. irradiation time for the second-order reaction kinetics. Blue line (5 mL 30% H_2O_2 solution), red line (10 mL 30% H_2O_2 solution), and green line (15 mL 30% H_2O_2 solution). (**A**) = 5 ppm MB solution, (**B**) = 10 ppm MB solution, (**C**) = 15 ppm MB solution.

Table 1 displays the correlation coefficient and the rate constant values achieved for MB degradation under UV irradiation for the zero, first, and second orders of reaction. The correlation coefficient values indicate that the data fit well with the zero-order kinetics.

Table 1. Correlation coefficient (R^2) and rate constant (k) values for the degradation of MB under UV irradiation for the zero, first, and second orders of reaction.

Process Conditions	Zero-Order Kinetics (C_t/C_o) vs. Time		First-Order Kinetics Ln (C_t/C_o) vs. Time		Second-Order Kinetics $1/(C_t/C_o)$ vs. Time	
5 ppm MB solution (100 mL)	R^2	k, min^{-1}	R^2	k, min^{-1}	R^2	k, min^{-1}
5 mL 30% H_2O_2	0.9057	0.0028	0.8528	0.0032	0.7980	0.0066
10 mL 30% H_2O_2	0.8963	0.0046	0.8245	0.0055	0.6000	0.0157
15 mL 30% H_2O_2	0.8744	0.0078	0.7100	0.0109	0.7981	0.0370
10 ppm MB solution (100 mL)	R^2	k, min^{-1}	R^2	k, min^{-1}	R^2	k, min^{-1}
5 mL 30% H_2O_2	0.9515	0.0047	0.8520	0.0050	0.7880	0.0130
10 mL 30% H_2O_2	0.9055	0.0068	0.8528	0.0108	0.7985	0.0160
15 mL 30% H_2O_2	0.9143	0.0082	0.8245	0.0128	0.7980	0.0217
15 ppm MB solution (100 mL)	R^2	k, min^{-1}	R^2	k, min^{-1}	R^2	k, min^{-1}
5 mL 30% H_2O_2	0.9059	0.0075	0.8750	0.0106	0.7988	0.0155
10 mL 30% H_2O_2	0.9459	0.0080	0.8850	0.0136	0.8146	0.0226
15 mL 30% H_2O_2	1.0000	0.0100	0.8528	0.0183	0.9063	0.0362

3.4. Photodegradation Mechanism

Several studies have concluded that adding H_2O_2 to the reaction system significantly improves MB degradation due to the generation of OH radicals [7–17,19–21]. The photodegradation of MB with H_2O_2 and UV irradiation is believed to work as per the following reaction schemes [50,51]. Initially, the H_2O_2 under UV irradiation produces OH radicals ($OH^{\bullet}$), which attack MB molecules and produce MB radicals ($MB^{\bullet}$). These MB radicals further undergo oxidation and finally convert to the intermediates CO_2 and H_2O. This reaction scheme advocates that the critical part is the generation of hydroxyl radicals from the photolysis of H_2O_2 molecules that react with the organic molecules. In addition, the $O_2^{\bullet -}$ species also attack MB molecules and degrade them into intermediates, CO_2 and H_2O. The reaction mechanism is given below. The complete reaction mechanism using the UV/H_2O_2 system is illustrated in Figure 7.

$$H_2O_2 + h\nu \rightarrow OH \quad (1)$$

$$2H_2O_2 \rightarrow 2H_2O + O_2 \quad (2)$$

$$e^- + H_2O_2 \rightarrow OH^{\bullet} + OH^- \quad (3)$$

$$h^+ + OH^- \rightarrow OH^{\bullet} \quad (4)$$

$$e^- + O_2 \rightarrow O_2^{\bullet -} \quad (5)$$

$$OH^{\bullet} + MB \rightarrow \text{Intermediates} + CO_2 + H_2O \quad (6)$$

$$O_2^{\bullet -} + MB \rightarrow \text{Intermediates} + CO_2 + H_2O \quad (7)$$

Table 2 presents a performance summary of different types of nanomaterials used for MB photodegradation in the literature along with the results of our study. The results obtained in our study are comparable and even better than most of the results provided in the literature.

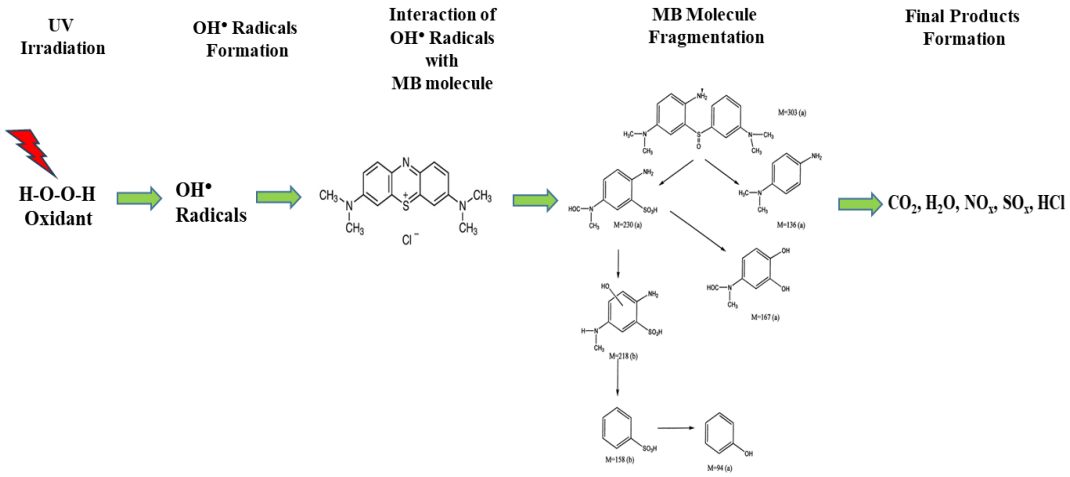

Figure 7. Mechanism of MB photodegradation using UV/H_2O_2 in the absence of a catalyst. Where (a) detected by GC/MS and (b) detected by LC/MS.

Table 2. Performance of nanomaterials used for MB photodegradation and comparison with our results.

No.	Catalyst Type	Irradiation Type	Degradation Efficiency, %	Irradiation Time, Min	Ref.
1	$CuWO_4$ NPs	sunlight	70	240	[10]
2	rGO-Fe_3O_4-TiO_2 (1:1:2) NCs	visible light	87	9	[17]
3	rGO-Fe_3O_4-TiO_2 (1:1:2) NCs	UV light	90	6	[17]
4	WO_3/$NiWO_4$ (having 20 wt% Ni) NCs	UV light	90	80	[29]
5	MgO NPs	visible light	90	120	[30]
6	Bi_2O_3/$MoSe_2$ NCs	visible light	96	80	[31]
7	CuO/CuS/MnO_2 NCs	visible light	98	160	[32]
8	Ag NPs	sunlight	80	120	[35]
9	ZnO/CuO/Al_2O_3(3:1:1) NCs	sunlight	98	15	[36]
10	TiO_2/3.0 wt% N-doped carbon quantum dots	visible light	93	60	[37]
11	$Co_{0.5}Zn_{0.5}MgFeO_4$	visible light	100	60	[40]
12	CNFO/g-C_3N_4	sunlight	97	180	[41]
13	$SrAl_2O_4$:$Eu^{2+}Dy^{3+}$/g-C_3N_4@NH_2-UiO-66	visible light	100	30	[42]
14	Co-SnO_2/sulfur-doped graphitic carbon nitride (50%) NCs	sunlight	96	150	[44]
15	ZnO@ olive fruit extract NPs	sunlight	75	180	[46]
16	UiO-66/g-C_3N_4	visible light	100	240	[52]
17	UV/H_2O_2 system	UV light	99	80	this work

4. Conclusions

This study demonstrated the efficient photodegradation of MB using H_2O_2 as an oxidant in the presence of UV irradiation. The effects of the concentrations of MB and H_2O_2 in the irradiated solution are examined. The following conclusions can be drawn from this study: MB degradation in the presence of H_2O_2 is not observed in the dark. MB degradation decreased in the presence of a higher initial concentration of MB in the reacting solution but increased with a higher concentration of H_2O_2 in the reacting solution. After the optimal H_2O_2 concentration was attained, the degradation time decreased with rising

H_2O_2 concentration. At this instant, the rate of degradation became inversely proportional to H_2O_2 concentration, as it started to scavenge the produced hydroxyl radicals. The oxidation process was facilitated with the proper addition of H_2O_2 and an optimum duration of exposure to UV radiation, therefore increasing the concentrations of MB and H_2O_2 which enhanced the degradation efficiency. The experimental data obtained are well-fitted with the zero-order reaction kinetics, as evident from the higher values of the correlation coefficient. It is anticipated that the OH radicals ($OH^{\bullet}$) generated during the breakdown of H_2O_2 and the $O_2^{\bullet-}$ species attack the MB molecules and produce MB radicals ($MB^{\bullet}$). These MB radicals undergo an oxidation reaction and convert to intermediates and finally to CO_2 and H_2O. The UV/H_2O_2 system proved quite efficient for the MB photodegradation of low-MB-concentration aqueous solutions without using a solid catalyst, and this system can be employed to degrade other organic dyes and drug pollutants present in industrial wastewater. Future studies should be conducted using batch and continuous stirred reactors, in natural sunlight, as well as in UV and visible lights of different wavelengths and intensities. It is also recommended to perform accelerated photodegradation using lasers.

Author Contributions: Conceptualization, M.A.A.; data curation, I.Y.Q.; formal analysis, M.A.A.; funding acquisition, I.M.M.; investigation, M.A.A.; methodology, I.M.M.; resources, I.M.M.; software, I.Y.Q.; validation, I.Y.Q.; writing—original draft, M.A.A.; writing—review and editing, I.M.M. All authors have read and agreed to the published version of the manuscript.

Funding: The research was funded by the Deputyship for Research & Innovation, Ministry of Education in Saudi Arabia through project number ISP23-58.

Institutional Review Board Statement: Not applicable.

Data Availability Statement: The data presented in this study are available from the corresponding author upon reasonable request.

Acknowledgments: The authors extend their appreciation to the Deputyship for Research & Innovation, Ministry of Education in Saudi Arabia for funding this research work through project number ISP23-58.

Conflicts of Interest: The authors declare no conflicts of interest.

References

1. Khan, I.; Saeed, K.; Zekker, I.; Zhang, B.; Hendi, A.H.; Ahmad, A.; Ahmad, S.; Zada, N.; Ahmad, H.; Shah, L.A.; et al. Review on Methylene Blue: Its Properties, Uses, Toxicity and Photodegradation. *Water* **2022**, *14*, 242. [CrossRef]
2. Oladoye, P.O.; Ajiboye, T.O.; Omotola, E.O.; Oyewola, O.J. Methylene Blue Dye: Toxicity and Potential Elimination Technology from Wastewater. *Results Eng.* **2022**, *16*, 100678. [CrossRef]
3. Zhu, T.; Ye, X.; Zhang, Q.; Hui, Z.; Wang, X.; Chen, S. Efficient Utilization of Photogenerated Electrons and Holes for Photocatalytic Redox Reactions using Visible Light-Driven Au/$ZnIn_2S_4$ Hybrid. *J. Hazard. Mater.* **2019**, *367*, 277–285. [CrossRef]
4. Phuc, N.H.; Lin, T.H.; Viet, T.Q.Q.; Nam, N.T.H.; Dat, N.M.; Hung, P.N.P.; Dat, N.T.; Minh, D.T.C.; Giang, N.T.H.; Huong, Q.T.T.; et al. Photodegradation of Methylene Blue and Photoproduction of Hydrogen Peroxide Using Magnesium Ferrite-Titanium Dioxide/Reduced Graphene Oxide as a Photo-Catalyst Under Visible Light. *Opt. Mater.* **2023**, *139*, 113832. [CrossRef]
5. Ersöz, E.; Yildirim, A.O. Green Synthesis and Characterization of Ag-Doped ZnO Nanofibers for Photodegradation of MB, RhB and MO Dye Molecules. *J. Korean Ceram. Soc.* **2022**, *59*, 655–670. [CrossRef]
6. Mohammed, H.A.; Khaleefa, S.A.; Basheer, M.I. Photolysis of Methylene Blue Dye Using an Advanced Oxidation Process (Ultraviolet Light and Hydrogen Peroxide). *J. Eng. Sustain. Dev.* **2021**, *25*, 59–67. [CrossRef]
7. Cao, Y.; Ren, Y.; Zhang, J.; Xie, T.; Lin, Y. Activation of H_2O_2 by Photo-Generated Electrons for Enhanced Visible Light Driven Methylene Blue Degradation with $ZnFe_2O_4$/$BiVO_4$ Heterojunction. *Opt. Mater.* **2021**, *121*, 111637. [CrossRef]
8. Mohammadzadeh, A.; Khoshghadam-Pireyousefan, M.; Shokrianfard-Ravasjan, B.; Azadbeh, M.; Rashedi, H.; Dibazar, M.; Mostafaei, A. Synergetic Photocatalytic Effect of High Purity ZnO Pod Shaped Nanostructures with H_2O_2 on Methylene Blue Dye Degradation. *J. Alloys Compd.* **2020**, *845*, 156333. [CrossRef]
9. El-Sheshtawy, H.S.; Ghubish, Z.; Shoueir, K.R.; El-Kemary, M. Activated H_2O_2 on Ag/SiO_2–$SrWO_4$ Surface for Enhanced Dark and Visible-Light Removal of Methylene Blue and p-Nitrophenol. *J. Alloys Compd.* **2020**, *842*, 155848. [CrossRef]
10. Waimbo, M.; Anduwan, G.; Renagi, O.; Badhula, S.; Michael, K.; Park, J.; Senthilkumar, V.; Kim, Y.S. Improved Charge Separation Through H_2O_2 Assisted Copper Tungstate for Enhanced Photocatalytic Efficiency for the Degradation of Organic Dyes Under Simulated Sun Light. *J. Photochem. Photobiol. B Biol.* **2020**, *204*, 111781. [CrossRef] [PubMed]

11. Wang, D.; Zhao, P.; Yang, J.; Xu, G.; Yang, H.; Shi, Z.; Hu, Q.; Dong, B.; Guo, Z. Photocatalytic Degradation of Organic Dye and Phytohormone by a Cu(II) Complex Powder Catalyst with Added H_2O_2. *Colloids Surf. A Physicochem. Eng. Asp.* **2020**, *603*, 125147. [CrossRef]
12. Shi, X.; Yu, Y.; Yang, Q.; Hong, X. Carboxyl Groups as Active Sites for H_2O_2 Decomposition in Photodegradation over Graphene Oxide/Polythiophene Composites. *Appl. Surf. Sci.* **2020**, *524*, 146397. [CrossRef]
13. Zhang, D.; Dai, F.; Zhang, P.; An, Z.; Zhao, Y.; Chen, L. The Photodegradation of Methylene Blue in Water with PVDF/GO/ZnO Composite Membrane. *Mater. Sci. Eng. C* **2019**, *96*, 684–692. [CrossRef]
14. Wang, X.; Li, D.; Nan, Z. Effect of N Content in g-C3N4 as Metal-Free Catalyst on H_2O_2 Decomposition for MB Degradation. *Sep. Purif. Technol.* **2019**, *224*, 152–162. [CrossRef]
15. Liu, J.; Asan, O.; Li, Z.; Wu, Z.; Zhu, K.; Zhuang, J.; Xi, Q.; Hou, Y.; Chen, J.; Cong, M.; et al. Jiankang Chen, Mengqi Cong, Jun Li, Guoming Qian, Zixia Lin. Photo-Fenton Reaction and H_2O_2 Enhanced Photocatalytic Activity of α-Fe_2O_3 Nanoparticles Obtained by a Simple Decomposition Route. *J. Alloys Compd.* **2019**, *771*, 398–405. [CrossRef]
16. Kalam, A.; Al-Sehemi, A.G.; Assiri, M.A.; Du, G.; Ahmad, T.; Ahmad, I.; Pannipara, M. Modified Solvothermal Synthesis of Cobalt Ferrite ($CoFe_2O_4$) Magnetic Nanoparticles Photocatalysts for Degradation of Methylene Blue with H_2O_2/Visible Light. *Results Phys.* **2018**, *8*, 1046–1053. [CrossRef]
17. Banerjee, S.; Benjwal, P.; Singh, M.; Kar, K.K. Graphene Oxide (rGO)-Metal Oxide (TiO_2/Fe_3O_4) Based Nanocomposites for the Removal of Methylene Blue. *Appl. Surf. Sci.* **2018**, *439*, 560–568. [CrossRef]
18. Liu, T.; Li, X.; Yuan, X.; Wang, Y. Enhanced Visible-Light Photocatalytic Activity of a TiO_2 Hydrosol Assisted by H_2O_2: Surface Complexation and Kinetic Modeling. *J. Mol. Catal. A Chem.* **2016**, *414*, 122–129. [CrossRef]
19. Gao, F.; Zhu, L.; Wang, Y.; Xie, H.; Li, J. Room Temperature Facile Synthesis of Cu_2Se Hexagonal Nanoplates Array Film and Its High Photodegradation Activity to Methyl Blue with the Assistance of H_2O_2. *Mater. Lett.* **2016**, *183*, 425–428. [CrossRef]
20. Zhang, Q.; Li, C.; Li, T. Rapid Photocatalytic Decolorization of Methylene Blue Using High Photon Flux UV/TiO_2/H_2O_2 Process. *J. Chem. Eng.* **2013**, *217*, 407–413. [CrossRef]
21. Shu, Z.; Bolton, J.R.; Belosevic, M.; Gamal El Din, M. Photodegradation of Emerging Micropollutants Using the Medium-Pressure UV/H_2O_2 Advanced Oxidation Process. *Water Res.* **2013**, *47*, 2881–2889. [CrossRef]
22. Jiang, G.; Zheng, X.; Wang, Y.; Li, T.; Sun, X. Photo-Degradation of Methylene Blue by Multi-Walled Carbon Nanotubes/TiO_2 Composites. *Powder Technol.* **2011**, *207*, 465–469. [CrossRef]
23. Yao, J.; Wang, C. Decolorization of Methylene Blue with TiO_2 Sol via UV Irradiation Photocatalytic Degradation. *Int. J. Photoenergy* **2010**, *2010*, 643182. [CrossRef]
24. Pouretedal, H.R.; Kadkhodaie, A. Synthetic CeO_2 Nanoparticle Catalysis of Methylene Blue Photodegradation: Kinetics and Mechanism. *Chin. J. Catal.* **2010**, *31*, 1328–1334. [CrossRef]
25. Zou, J.; Gao, J.; Xie, F. An Amorphous TiO_2 Sol Sensitized with H_2O_2 with the Enhancement of Photocatalytic Activity. *J. Alloys Compd.* **2010**, *497*, 420–427. [CrossRef]
26. Andronic, L.; Duta, A. Influence of pH and H_2O_2 on Dyes Photodegradation. *Phys. Status Solidi C* **2008**, *5*, 3332–3337. [CrossRef]
27. Banat, F.; Al-Asheh, S.; Al-Rawashdeh, M.; Nusair, M. Photodegradation of Methylene Blue Dye by the UV/H_2O_2 and UV/Acetone Oxidation Processes. *Desalination* **2005**, *181*, 225–232. [CrossRef]
28. Bessy, T.C.; Sarojoni, V.; Johnson, J.B.; Bakri, M.M.; Manna, C.E.; Florence, S.S.; Bindhu, M.R. Optical, Structural, Morphological, Antibacterial, and Photodegradation Characteristics of $Ba_xMg_{0.8-x}Fe_2O_4$ (x = 0.2, 0.4, and 0.6) Nanocrystalline Powders Synthesized by Combustion Method. *Phys. Status Solidi A Appl. Mater. Sci.* **2022**, *219*, 202200366. [CrossRef]
29. Ahmad, A.; Khan, M.; Khan, S.; Luque, R.; Almutairi, T.M.; Karami, A.M. A Facile Co-Precipitation Synthesis of Novel $WO_3/NiWO_4$ Nanocomposite with Improved Photocatalytic Activity. *Mater. Sci. Semicond.* **2021**, *133*, 105970. [CrossRef]
30. Ahmad, A.; Khan, M.; Khan, S.; Luque, R.; Almutairi, T.M.; Karami, A.M. Bio-Construction of MgO Nanoparticles Using Texas Sage Plant Extract for Catalytical Degradation of Methylene Blue via Photocatalysis. *Int. J. Environ. Sci. Technol.* **2023**, *20*, 1451–1462. [CrossRef]
31. Alahmadi, M.; Alsaedi, W.H.; Mohamed, W.S.; Hassan, H.M.A.; Ezzeldien, M.; Abu-Dief, A.M. Development of $Bi_2O_3/MoSe_2$ Mixed Nanostructures for Photocatalytic Degradation of Methylene Blue Dye. *J. Taibah Univ. Sci.* **2023**, *17*, 2161333. [CrossRef]
32. Abdullah, M.; John, P.; Ashiq, M.N.; Manzoor, S.; Ghori, M.I.; Nisa, M.U.; Abid, A.G.; Butt, K.Y.; Ahmed, S. Development of CuO/CuS/MnO_2 Ternary Nanocomposite for Visible Light-Induced Photocatalytic Degradation of Methylene Blue. *Nanotechnol. Environ. Eng.* **2023**, *8*, 63–73. [CrossRef]
33. Zyoud, S.H.; Yahia, I.S.; Shahwan, M.; Zyoud, A.; Zahran, H.Y.; Abdelwahab, M.S.; Daher, M.G.; Nasor, M.; Makhadmeh, G.N.; Hassan, N.; et al. Fast and Excellent Enhanced Photocatalytic Degradation of Methylene Blue Using Silver-Doped Zinc Oxide Submicron Structures Under Blue Laser Irradiation. *Crystals* **2023**, *13*, 229. [CrossRef]
34. Zhao, X.; Wang, C.; Chou, N.-N.; Wang, F.-H.; Yang, C. Synthesis of ZnO Nanoflower Arrays on Patterned Cavity Substrate and Their Application in Methylene Blue Degradation. *Materials* **2023**, *16*, 2647. [CrossRef]
35. Basalius, H.; Mani, A.; Amalanathan, M.; Mary, M.; Lenin, M.; Parvathiraja, C.; Siddiqui, M.R.; Wabaidur, S.M.; Islam, M.M. Green Synthesis of Nano-Silver Using *Syzygium samarangense* Flower Extract for Multifaceted Applications in Biomedical and Photocatalytic Degradation of Methylene Blue. *Appl. Nanosci.* **2023**, *13*, 3735–3747. [CrossRef]
36. Al-Attar, H.M.; Hussein, H.T.; Zamel, R.S.; Addie, A.J.; Mohammed, M.K.A. Methylene Blue Degradation Using ZnO:CuO:Al_2O_3 Nanocomposite Synthesized by Liquid Laser Ablation. *Opt. Quant. Electron.* **2023**, *55*, 309. [CrossRef]

37. Jin, Y.; Tang, W.; Wang, J.; Ren, F.; Chen, Z.; Sun, Z.; Ren, P. Construction of Biomass Derived Carbon Quantum Dots Modified TiO_2 Photocatalysts with Superior Photocatalytic Activity for Methylene Blue Degradation. *J. Alloys Compd.* **2023**, *932*, 167627. [CrossRef]
38. Elaiyappillai, E.; Elizabeth, I.B.; Wang, S.-F.; Lydia, I.S. Strontium Hexaferrite Microspheres: Synthesis, Characterization and Visible-Light-Driven Photocatalytic Activity Towards the Degradation of Methylene Blue Dye. *Opt. Mater.* **2023**, *137*, 113565. [CrossRef]
39. Fu, C.; Yan, M.; Wang, Z.; Ji, L.; Zhang, X.; Song, W.; Xu, Z.; Bhatt, K.; Wang, Z.; Zhu, S. New Insights into the Degradation and Detoxification of Methylene Blue Using Heterogeneous-Fenton Catalyzed by Sustainable Siderite. *Environ. Res.* **2023**, *216*, 114819. [CrossRef]
40. Chahar, D.; Kumar, D.; Thakur, P.; Thakur, A. Visible Light Induced Photocatalytic Degradation of Methylene Blue Dye by Using Mg Doped Co-Zn Nanoferrites. *Mater. Res. Bull.* **2023**, *162*, 112205. [CrossRef]
41. Waheed, I.F.; Hamad, M.A.; Jasim, K.A.; Gesquiere, A.J. Degradation of Methylene Blue Using a Novel Magnetic $CuNiFe_2O_4$/g-C_3N_4 Nanocomposite as Heterojunction Photocatalyst. *Diam. Relat. Mater.* **2023**, *133*, 109716. [CrossRef]
42. Chen, M.-L.; Li, S.; Wen, L.; Xu, Z.; Li, H.; Li, D.; Cheng, Y.-H. Exploration of Double Z-type Ternary Composite Long-Afterglow/Graphitic Carbon Nitride@Metal–Organic Framework for Photocatalytic Degradation of Methylene Blue. *J. Colloid Interface Sci.* **2023**, *629*, 409–421. [CrossRef]
43. Sun, Q.; Huang, S.; Li, Z.; Su, D.; Sun, J. Synergistic Activation of Persulfate by Heat and Cobalt-Doped-Bimetallic-MOFs for Effective Methylene Blue Degradation: Synthesis, Kinetics, DFT Calculation, and Mechanisms. *J. Environ. Chem. Eng.* **2023**, *11*, 109065. [CrossRef]
44. Javed, M.; Iqbal, S.; Qamar, M.A.; Shariq, M.; Ahmed, I.A.; BaQais, A.; Alzahrani, H.; Ali, S.K.; Masmali, N.A.; Althagafi, T.M.; et al. Fabrication of Effective Co-SnO_2/SGCN Photocatalysts for the Removal of Organic Pollutants and Pathogen Inactivation. *Crystals* **2023**, *13*, 163. [CrossRef]
45. Fallatah, A.M.; Alahmari, S.D.; Farid, H.M.T. Facile Synthesis of the MOF Derived $ZnMn_2O_4$ Nanorods for Dyes Degradation in Water. *J. Mater. Sci. Mater. Electron.* **2023**, *34*, 1630. [CrossRef]
46. Hussain, S.; Alam, M.M.; Imran, M.; Ali, M.A.; Ahamad, T.; Haidyrah, A.S.; Alotaibi, S.M.A.R.; Naik, M.; Shariq, M. A facile low-cost scheme for highly photoactive Fe3O4-MWCNTs nanocomposite material for degradation of methylene blue. *Alex. Eng. J.* **2022**, *61*, 9107–9117. [CrossRef]
47. Negash, A.; Mohammed, S.; Weldekirstos, H.D.; Ambaye, A.D.; Gashu, M. Enhanced Photocatalytic Degradation of Methylene Blue Dye Using Eco-friendly Synthesized rGO@ZnO Nanocomposites. *Sci. Rep.* **2023**, *13*, 22234. [CrossRef]
48. Naffeti, M.; Zaïbi, M.A.; Nefzi, C.; García-Arias, A.V.; Chtourou, R.; Postigo, P.A. Highly Efficient Photodegradation of Methylene Blue by A Composite Photocatalyst of Bismuth Nanoparticles on Silicon Nanowires. *Environ. Technol. Innov.* **2023**, *30*, 103133. [CrossRef]
49. Ighalo, J.O.; Ajala, O.J.; Umenweke, G.; Ogunniyi, S.; Adeyanju, C.A.; Igwegbe, C.A.; Adeniyi, A.G. Mitigation of Clofibric Acid Pollution by Adsorption: A Review of Recent Developments. *J. Environ. Chem. Eng.* **2020**, *8*, 104264. [CrossRef]
50. Sugha, A.; Bhatti, M.S. Degradation of methylene blue dye by UV/H_2O_2 advanced oxidation process: Reaction kinetics, residual H_2O_2 and specific energy consumption evaluation. *Desalin. Water Treat.* **2022**, *274*, 297–307. [CrossRef]
51. Tantubay, K.; Das, P.; Baskey, M. Hydrogen peroxide–assisted photocatalytic dye degradation over reduced graphene oxide integrated $ZnCr_2O_4$ nanoparticles. *Environ. Sci. Pollut. Res.* **2022**, *29*, 17309–17318. [CrossRef] [PubMed]
52. Zhang, Y.; Zhou, J.; Feng, Q.; Chen, X.; Hu, Z. Visible Light Photocatalytic Degradation of MB using UiO-66/g-C3N4 Heterojunction Nanocatalyst. *Chemosphere* **2018**, *212*, 523–532. [CrossRef] [PubMed]